

DIRECT NUMERICAL SIMULATION OF SMOOTH AND ROUGH WALL TURBULENT BOUNDARY LAYERS WITH HEAT TRANSFER

F. Secchi¹, J. Yang¹, D. Gatti¹, A. Stroh¹, P. Schlatter², B. Frohnappel¹

¹Institute of Fluid Mechanics (ISTM), Karlsruhe Institute of Technology, Germany

²Chair of Fluid Mechanics, Friedrich-Alexander-Universität Erlangen-Nürnberg, Germany
francesco.secchi@kit.edu

INTRODUCTION

Boundary layers are ubiquitous as they form around any solid body moving relative to a fluid. By definition, heat and momentum are exchanged between the moving body and the free-stream flow within the boundary layer thickness. In most engineering applications, the flow within the boundary layer is turbulent, and the surface over which the boundary layer develops is rough. Even though many aspects on the nature of turbulent boundary layers over smooth walls are currently well-established, a greater understanding gap is still present when surface roughness comes into play. Rough wall-bounded turbulence has been extensively studied in the literature, but only a limited number of investigations address spatially developing rough wall flows and experimental efforts on the topic are not equally supported by high fidelity numerical studies [1, 2]. In fact, due to the extensive computational demands required to simulate such flows, just a few investigations in the literature report studies of rough wall turbulent boundary layers and, most of available results are limited to momentum transfer and little is known regarding heat transfer [3, 4, 5, 6].

In this study we present direct numerical simulation (DNS) results of smooth and rough wall zero pressure gradient turbulent boundary layers with heat transfer. The boundary layer develops along a smooth plate before entering a region with homogeneous surface roughness. The plate is kept at a constant and uniform temperature, which is greater than the temperature of the free-stream flow. The study assesses the effects of surface roughness by comparing mean flow statistics with smooth wall turbulent boundary layer data obtained using the same DNS framework.

PROBLEM FORMULATION

The incompressible Navier-Stokes equations are numerically integrated using the pseudo-spectral flow solver SIMSON [7], in which Fourier space and Chebyshev polynomials are used for discretizing flow variables in the wall-parallel and wall-normal directions, respectively. The domain of the simulations is sketched in figure 1. The computational box has size $L_x = 3000\delta_{1,in}$, $L_z = 124\delta_{1,in}$, and $L_y = 100\delta_{1,in}$ in the streamwise, spanwise and wall-normal directions, respectively. Here $\delta_{1,in}$ indicates the displacement thickness of the Blasius boundary layer at the inlet section of the computational domain. A homogeneous surface roughness patch of length $L_R = 2350\delta_{1,in}$ is laid over the bottom wall of the computational domain starting at $x = L_T = 150\delta_{1,in}$. A sigmoid

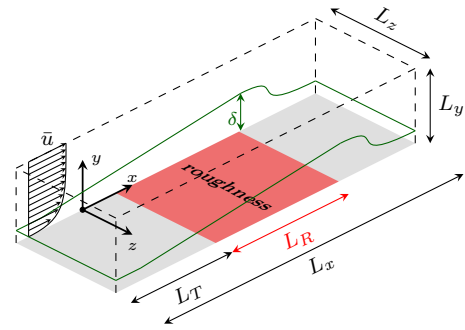


Figure 1: View of the computational domain. The red area represents the region where surface roughness is present. The aspect ratio of the figure is not representative of the actual simulation.

scaling function is employed on the roughness height distribution in the vicinity of $x = L_T$ to facilitate a gradual transition from smooth to rough wall. The length L_T is designed to reach a turbulent state at the beginning of the roughness patch that is independent on the tripping used to make the boundary layer turbulent. Periodic boundary conditions are applied in both wall-parallel directions for all flow variables. To cope with the flow development in the streamwise direction, the re-scaling strategy presented in [7] is applied. No-slip and no-penetration boundary conditions are applied at the bottom wall using an immersed boundary method based on the method of [8]. A similar approach is applied to enforce a Dirichlet boundary condition for the temperature field with a uniform temperature T_w . On the top plane of the computational domain, the velocity field is prescribed to match the free-stream velocity u_∞ in the streamwise direction and allowed to have transpiration in the wall-normal direction [7]. On the other hand, the temperature is prescribed to be that of the free-stream flow T_∞ , with $T_\infty < T_w$. The Prandtl number is set to $Pr = 1$.

Surface roughness is a filtered three-dimensional scan of a real sandpaper rough surface. The characteristic size k of the roughness topography is defined to be $k_t = 4\delta_{1,in}$, where k_t is the peak-to-trough height of the roughness.

RESULTS

The friction coefficient $C_f = 2\tau_w/(\rho u_\infty^2)$ and Stanton number $St = 2q_w/(\rho c_p u_\infty \Delta T)$ distributions for the smooth and

rough wall cases are shown in figure 2. Here τ_w is the wall-shear stress, q_w the wall-heat flux, ρ is the fluid density, c_p is the heat capacity at constant pressure, and $\Delta T = T_w - T_\infty$. The skin friction coefficient and Stanton number attain very similar values along the boundary layer, except for the rough wall case near the roughness leading edge (approximately for $x < 500\delta_{1,in}$). In this region, the rough wall induced increase in skin friction exceeds significantly the wall-heat flux enhancement. This is consistent with the pressure drag introduced by roughness elements which does not play a direct role in increasing the wall-heat flux. Compared to the smooth-wall case, skin-friction and Stanton number decrease faster along the boundary layer and, for $x > 1500\delta_{1,in}$, a local net decrease is observed in both the skin-friction coefficient and Stanton number for the rough wall case.

The roughness Reynolds number $k^+ = k/\delta_\nu$ (a plus superscript indicates viscous units scaled quantities, δ_ν indicates the viscous length scale and ν is the kinematic viscosity), is reported in figure 3. In the same figure, the boundary layer thickness is also shown in terms of displacement δ_1 , momentum δ_2 and thermal-energy δ_T thickness. k^+ ranges from approximately $k^+ = 200$ close to the roughness leading edge to approximately $k^+ = 40$ near the end of the roughness region. As such, the flow moves from a fully-rough to a transitionally rough condition along the boundary layer. As a result of this flow transition, viscous units scaled mean velocity and temperature profiles at different streamwise locations, which are reported in figure 4, display a visible scatter compared to the smooth wall case mean profiles.

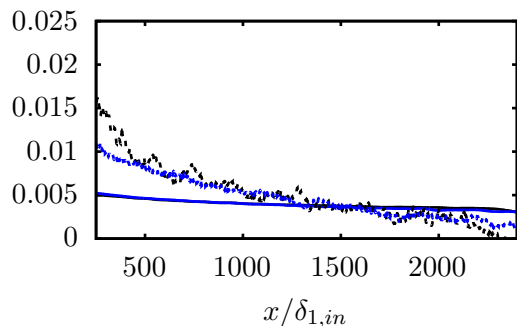


Figure 2: Friction coefficient and Stanton number distributions along the boundary layer. Smooth wall: —, C_f ; —, St . Rough wall: - - - - , C_f ; - - - - , St .

ACKNOWLEDGEMENTS

We greatly acknowledge the support by the German Research Foundation (DFG) under the Collaborative Research Centre TRR150 (project number 237267381). The simulations presented in this work were performed on the HPE Apollo (Hawk) supercomputer at the High Performance Computing Center Stuttgart (HLRS) under the grant number zzz44198.

REFERENCES

- [1] D. Chung, N. Hutchins, M. Schultz, and K. Flack, “Predicting the drag of rough surfaces,” *Annual Review of Fluid Mechanics*, vol. 53, no. 1, pp. 439–471, 2021.
- [2] M. Kadivar, D. Tormey, and G. McGranaghan, “A review on turbulent flow over rough surfaces: Fundamentals and

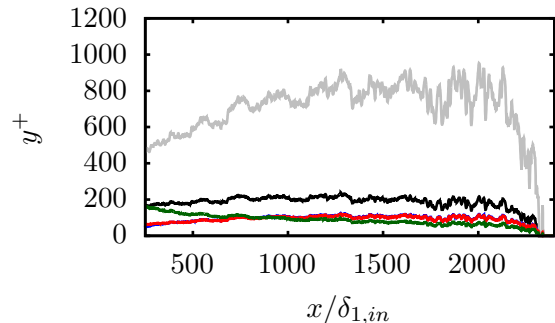


Figure 3: Roughness Reynolds number and boundary layer thicknesses distributions along the rough wall boundary layer. —, δ_{99}^+ ; —, δ_1^+ ; —, δ_2^+ ; —, δ_T^+ ; —, k^+ .

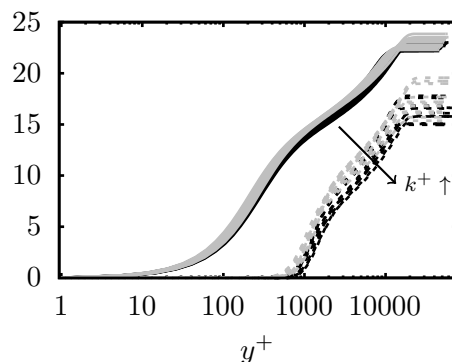


Figure 4: Viscous units scaled mean velocity and temperature profiles. Smooth wall: —, $\langle \bar{u} \rangle^+$; —, $(T_w - \langle \bar{T} \rangle)^+$. Rough wall: - - - - , $\langle \bar{u} \rangle^+$; - - - - , $(T_w - \langle \bar{T} \rangle)^+$.

theories,” *International Journal of Thermofluids*, vol. 10, p. 100077, 2021.

- [3] J. Cardillo, Y. Chen, G. Araya, J. Newman, K. Jansen, and L. Castillo, “DNS of a turbulent boundary layer with surface roughness,” *Journal of Fluid Mechanics*, vol. 729, p. 603–637, 2013.
- [4] J. Yuan and U. Piomelli, “Numerical simulation of a spatially developing accelerating boundary layer over roughness,” *Journal of Fluid Mechanics*, vol. 780, p. 192–214, 2015.
- [5] A. Doosttalab, G. Araya, J. Newman, R. Adrian, K. Jansen, and L. Castillo, “Effect of small roughness elements on thermal statistics of a turbulent boundary layer at moderate reynolds number,” *Journal of Fluid Mechanics*, vol. 787, p. 84–115, 2016.
- [6] I. K. Kaminaris, E. Balaras, M. P. Schultz, and R. J. Volino, “Secondary flows in turbulent boundary layers developing over truncated cone surfaces,” *Journal of Fluid Mechanics*, vol. 961, p. A23, 2023.
- [7] M. Chevalier, P. Schlatter, A. Lundbladh, and D. Henningson, “SIMSON–A pseudo-spectral solver for incompressible boundary layer flow.,” *Technical Report TRITA-MEK*, pp. 1–100, 2007.
- [8] D. Goldstein, R. Handler, and L. Sirovich, “Modeling a no-slip flow boundary with an external force field,” *Journal of Computational Physics*, vol. 105, no. 2, pp. 354–366, 1993.